

Tuning of intervalence charge transfer energies by substituents in one-dimensional bis(triarylamine) systems

2 PERKIN

Christoph Lambert* and Gilbert Nöll

Institut für Organische Chemie, Bayerische Julius-Maximilians-Universität Würzburg, Am Hubland, D-97074 Würzburg, Germany. E-mail: lambert@chemie.uni-wuerzburg.de

Received (in Cambridge, UK) 7th August 2002, Accepted 24th October 2002

First published as an Advance Article on the web 13th November 2002

We synthesised a series of linear bis(triarylamine) species whose triarylamine redox centres have different local redox potentials which were tuned by substituents in the *para*-position. The mixed-valence (MV) radical cations of these systems were generated and investigated *in situ* by UV/Vis/NIR spectroelectrochemistry. The electronic coupling between the redox centres was analysed by the generalised Mulliken–Hush theory which gave a practically constant coupling. The radical cations of the species show an intervalence charge transfer (IV-CT) band in the NIR whose energy varies linearly with the electrochemical redox potential splitting. This correlation proves that the Marcus–Hush two-level model is an adequate way to describe the electronic situation in these linear MV systems.

Introduction

Triarylamines have been used as hole transport components in materials for optoelectronic applications such as photorefractive systems,¹ photovoltaic cells,² organic light emitting devices (OLED)³ *etc.* Besides these applications, triarylamines have been investigated as charge bearing units in one- and multi-dimensional systems for studying intramolecular adiabatic electron transfer.^{4–11} These systems in which two or more triarylamines are incorporated represent organic equivalents to the well known inorganic mixed-valence (MV) compounds.^{12–14} In contrast to inorganic MV species much less purely organic systems are known, among them bishydrazine species^{15,16} and quinones.¹⁷ The basic structure of a one-dimensional MV species based on triarylamines is sketched below.

There are a number of advantages in using triarylamines in MV compounds. First, triarylamines guarantee reversible redox behaviour as long as the *para*-positions of the phenyl rings are protected. This stability is due to the delocalisation of the positive charge and the spin within the triarylamine moiety.¹⁸ Second, the spacer between the two triarylamine redox centres can be varied over a broad range very easily. Third, the intervalence charge transfer (IV-CT) band associated with the optically induced hole transfer from one triarylamine centre to the other is usually quite intense and well separated from other bands so as to allow accurate band fits. Fourth, the redox potentials of the triarylamine centres can be tuned by substituents in the *para*-position.¹⁹ The investigation of the latter point is the focus of this paper.

The potential energy surfaces (PES) of one-dimensional MV compounds can be constructed by the two-state Marcus–Hush theory (see Fig. 1):^{14,20,21} two adiabatic functions are used to describe the states in which the hole is localised on the left-hand triarylamine moiety and on the right-hand triarylamine moiety, respectively. The potentials of these states along the ET (electron transfer) reaction coordinate x are given by quadratic functions which were, in our case, augmented by quartic functions.^{22,23} The force constant of the quadratic potential is λ , the Marcus reorganisation energy, which comprises the internal (vibrational) part and the solvent contribution. Although the

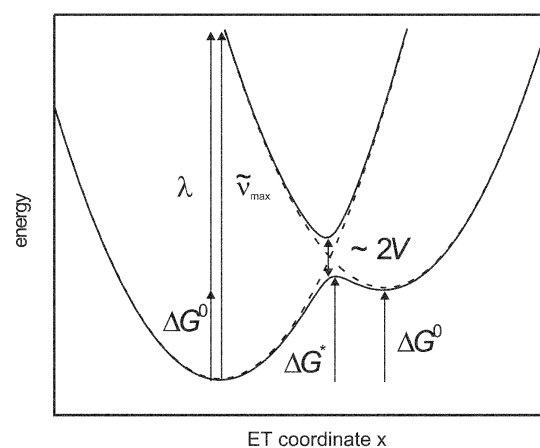


Fig. 1 Potential energy surfaces (solid lines) constructed from two diabatic potentials (dashed lines) using eqn. (1).

two diabatic states are not degenerate we assume equal force constants for both states in the present case. The quartic augmentation makes the adjustment of the potentials more flexible and is given by the asymmetry parameter C which has no direct physical meaning. These diabatic states are coupled in a 2×2 secular determinant (eqn. (1)) which results in two adiabatic potentials (see Fig. 1).

The strength of the electronic coupling is given by the coupling integral V . The ground state is a double-well PES if V is smaller than $\lambda/2$. In the case of a symmetrical MV compound the two minima of the double-well potential are degenerate. In the general case of asymmetrical MV compounds they differ in energy. This energy difference is introduced by an off-set of the diabatic potentials, ΔG^0 (see Fig. 1). Optical excitation from a minimum of the ground state PES to the excited state PES gives rise to an absorption band in the NIR, the so-called IV-CT band. If the parameter $C = 0$ and a Boltzmann distribution of ground state population is assumed, the resulting absorption band is exactly Gaussian-shaped with a distinct band-width at half-maximum at the high-temperature limit given by $\tilde{\nu}_{1/2}^{\text{HTL}} =$

$$\begin{vmatrix} \lambda(x^2(1+Cx^2))/(1+C) & V \\ V & \lambda((1-x)^2(1+C(x-1)^2))/(1+C) + \Delta G^0 \end{vmatrix} = 0 \quad (1)$$

Table 1 Redox potentials and differences of **1–4** in CH₂Cl₂–0.2 M TBAH vs. Fc/Fc⁺ at 250 mV s⁻¹

	$E_{1/2}(\text{M}/\text{M}^+)/\text{mV}^a$	$E_{1/2}(\text{M}^+/\text{M}^{2+})/\text{mV}^a$	$\Delta E_{1/2}/\text{mV}^b$	$\Delta E_{1/2} - \Delta E_{1/2}(\mathbf{1})/\text{mV}^b$
1	205	355	150	0
2	230	450	220	70
3	-5	365	370	220
4	290	830	540	390

^a ±5 mV, ^b ±7 mV.

47.94/λ.²¹ In practice, the observed IV-CT bands are often very asymmetric and broader than simple classical theory predicts: broader bands are observed if high-energy vibrations are coupled to the ET.²⁴ This effect is taken into account by the parameter *C* which makes the bands broader and slightly asymmetric. Stronger band asymmetries (a much steeper fall-off at the low-energy side of the IV-CT band) are due to cut-off effects.^{6,14,25} These cut-off effects are present if the ET barrier Δ*G*^{*} is much smaller than λ/4 which is the case if *V* is significant.

If *C* and *V* are small the IV-CT band energy $\tilde{\nu}_{\text{max}}$ equals the sum of λ and Δ*G*⁰. Thus, there should be a linear correlation between $\tilde{\nu}_{\text{max}}$ and Δ*G*⁰ in a series of compounds for which λ is constant which can safely be assumed for the triarylamine redox centres. The problem arises of how to determine Δ*G*⁰. Δ*G*⁰ reflects the relative tendency of a diabatic (localised) state to be charged. This relative tendency can be approximated by the redox potential difference Δ*E*_{1/2} of the processes **MV** → **MV**⁺ + e⁻ and **MV**⁺ → **MV**²⁺ + e⁻. This approach presumes that in a series of compounds *V* is constant because we have recently shown that Δ*E*_{1/2} is proportional to *V* for a series of bis(triarylamine) systems.⁶ In addition, the MV compounds must not undergo major reorganisation (*e.g.* bond stretching and twisting or ion pairing²⁶) upon doubly charging the molecule. The above mentioned correlation of Δ*E*_{1/2} vs. *V* indicates that reorganisational effects are indeed minor in triarylamine systems.

In inorganic MV compounds in which two metal redox centres are bridged by a bidentate ligand, Curtis *et al.*²⁸ as well as others²⁷ introduced asymmetry of the diabatic potentials by addition of different ligands to the two metal redox centres and a linear correlation of Δ*G*⁰ vs. Δ*E*_{1/2} was observed for Ru species in MeCN solvent with a slope of unity. These correlations cover a range of redox potential differences of *ca.* 250 mV. In the present investigation we will show that a similar correlation is also valid for purely organic MV species based on triaryl amines connected by a CC triple bond. The redox asymmetry of the compounds and, thus, Δ*G*⁰ was introduced by different substituents in the *para*-position of the triaryl amines: MeO, Me, Cl, CN.

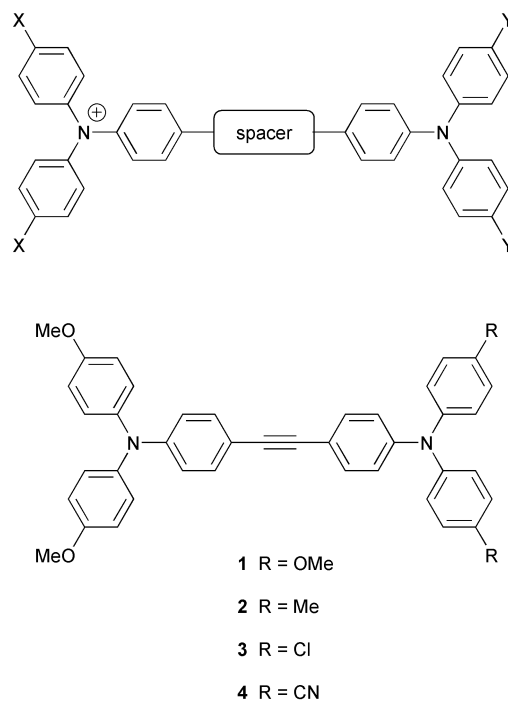
Results and discussion

The compounds **1–4** were synthesised by conventional Pd catalysed cross coupling reactions of haloarenes and terminal alkynes in moderate to good yields.

The redox potentials of **1–4** were measured in CH₂Cl₂–0.2 M TBAH by cyclic voltammetry. The redox potentials and their differences are given in Table 1. As expected, the relative redox potential splitting increases with increasing electron acceptor strength of the substituents *R* which makes the second oxidation more difficult.

For measurement of the IV-CT bands, the radical cations of **1–4** were generated *in situ* in a cell with an optically transparent thin-layer electrode (OTTLE) and their UV/Vis/NIR spectra were recorded during step-wise oxidation at a gold mini-grid working electrode. The spectra obtained are corrected for the comproportionation equilibrium⁴ and are given in Fig. 2.

The Vis/NIR spectra of **1**⁺–**4**⁺ are characterised by an intense



IV-CT band at *ca.* 6000–11000 cm⁻¹ and a band which is associated with a localised triarylamine radical cation excitation (so-called radical band) at *ca.* 13500 cm⁻¹.^{18,19} The IV-CT band and the radical band were deconvoluted by fitting each band with two Gaussian functions. In the case of **4**⁺ only one Gaussian function for each band was sufficient owing to strong band overlap.

From the deconvoluted IV-CT bands the coupling integral *V* was calculated by eqn. (2) which is derived from the generalised Mulliken–Hush theory^{29–31} where $\tilde{\nu}_{\text{max}}$ is the IV-CT band energy, μ_{eg} is the transition moment which was calculated by eqn. (3) from the integrated IV-CT band, Δ*μ*_{ab} is the diabatic dipole moment difference which was calculated by eqn. (4) from Δ*μ*_{gg}, the adiabatic dipole moment difference of the ground

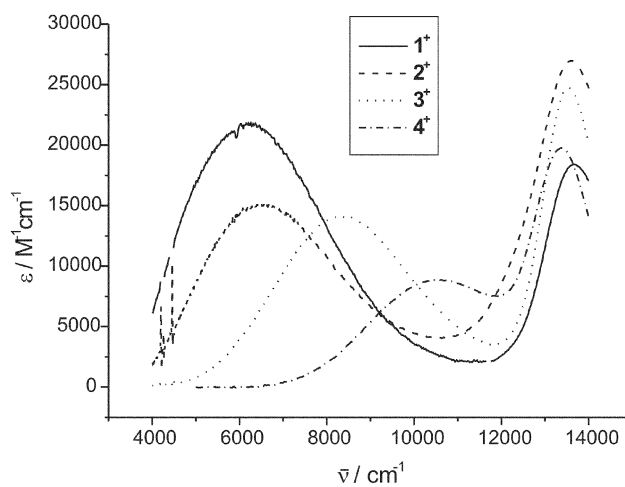
**Fig. 2** Vis/NIR spectra of **1**⁺–**4**⁺ in CH₂Cl₂–0.2 M TBAH.

Table 2 Optical data of the IV-CT bands and ET parameters obtained from the band fit by tuning the potential energy surface

	$\tilde{\nu}_{\max}^a/\text{cm}^{-1}$	$\varepsilon^b/\text{M}^{-1}\text{cm}^{-1}$	$\mu_{\text{eg}}^c/\text{D}$	V^d/cm^{-1}	λ/cm^{-1}	C	$\Delta G^0/\text{cm}^{-1}$	$\Delta G^*/\text{cm}^{-1}$
1⁺	6190	21900	11.7	1120	6300	0.10	0	550
2⁺	6490	15000	9.2	950	6300	0.05	400	910
3⁺	8260	14100	7.9	1060	6300	0.05	2000	1870
4⁺	10560	8900	5.4	940	6300 ^e	0.00	4200	—

^a $\pm 100\text{ cm}^{-1}$. ^b $\pm 1000\text{ M}^{-1}\text{ cm}^{-1}$. ^c $\pm 0.6\text{ D}$. ^d $\pm 70\text{ cm}^{-1}$. ^e Fixed. ^f $\pm 140\text{ cm}^{-1}$.

state, and μ_{eg} . $\Delta\mu_{\text{gg}} = er$ was estimated from the geometric distance of the nitrogen atoms, r , which was taken from an AM1 calculation.

$$V = \frac{\mu_{\text{eg}} \tilde{\nu}_{\max}}{\Delta\mu_{\text{ab}}} \quad (2)$$

$$\mu_{\text{eg}} = 0.09584 \sqrt{\int_{\tilde{\nu}_{\max}} \varepsilon(\tilde{\nu}) d\tilde{\nu}} \quad (3)$$

$$\Delta\mu_{\text{ab}} = \sqrt{(\Delta\mu_{\text{gg}})^2 + 4(\mu_{\text{eg}})^2} \quad (4)$$

The coupling integrals determined by eqn. (2) were used to construct the PES by eqn. (1). The parameters λ and C were tuned in order to get best fit to the experimental IV-CT band at the high-energy side. For **2⁺** the fit is given in Fig. 3. The resulting optical and ET parameters are collected in Table 2.

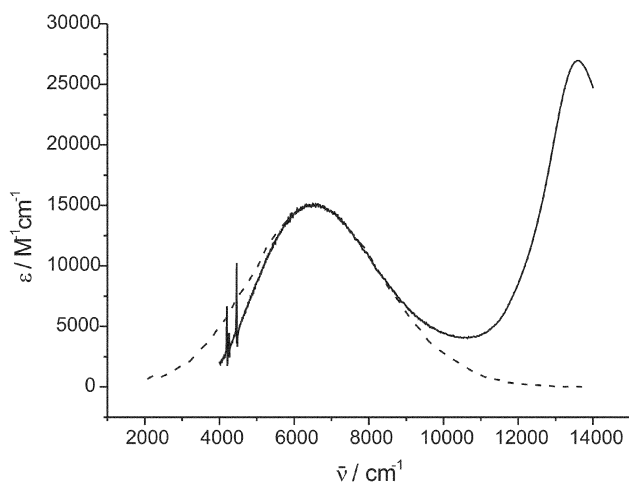


Fig. 3 IV-CT band of **2⁺** (solid line) and fit (dashed line).

From Figs. 2 and 3 and the data in Table 2 it is obvious that the IV-CT bands of **1⁺–3⁺** (for **4⁺** definite conclusions are prohibited because of strong band overlap) are asymmetric with a much steeper fall-off at the low-energy side than the band simulation predicts. As mentioned above, this asymmetry (cut-off effect) is due to the relatively strong coupling and has been studied in detail in ref. 6. On the other hand, for **1⁺** the parameter $C = 0.1$ shows that the band at the high-energy side is somewhat broader as simple Hush theory predicts for the high-temperature limit. The IV-CT band becomes more symmetric (and C approaches zero) when the ET barrier ΔG^* rises (**2⁺ → 4⁺**).

A major assumption for the validity of a correlation of $\tilde{\nu}_{\max}$ with ΔG^0 is that the coupling V remains constant within the series of MV compounds. The average for **1⁺–4⁺** is $V = 1020 \pm 50\text{ cm}^{-1}$ for all four compounds. This observation is reasonable because the conjugation path between the two redox centres is the same in all species. However, we have to stress that we used the same effective adiabatic ET distance r (for which we took

the geometric NN-distance = $12.5\text{ \AA} \triangleq 59.9\text{ D}$) for all species **1⁺–4⁺** for estimating the adiabatic transition moment difference $\Delta\mu_{\text{gg}}$ in eqn. (4) although it might be possible that r is different owing to different substituents being attached to the phenyl rings. These substituents will lead to a deviation of the average centre of positive charge distribution in the triarylamine radical cation moiety from the geometric position of the nitrogen atom. To assess this factor we performed semiempirical UHF AM1 optimisations of the radical cation of **1** and of a model compound *N,N,N',N'*-tetrakis(*p*-cyanophenyl)tolane-4,4'-diamine **5**. These computations gave the dipole moment of the radical cation species with the centre of mass as the vector origin.^{32,33} Twice the dipole moment then equals the adiabatic dipole moment difference $\Delta\mu_{\text{gg}}$ which is 54.0 D for **1⁺** and 45.2 D for **5⁺**. The average (49.6 D) should be a good estimate for the dipole moment difference of **4⁺** which cannot be calculated directly. With these dipole moments $V(\mathbf{1}^+)$ rises by 9% to 1220 cm^{-1} and $V(\mathbf{4}^+)$ by 20% to 1130 cm^{-1} . However, both couplings are still within experimental error the same. Thus, our assumption of a fairly constant V throughout the series is reasonable.

According to our PES fit (see Table 2) the total reorganisation energy λ of **1⁺–3⁺** is constant (6300 cm^{-1}). This value was kept fixed for **4⁺** where strong band overlap of the IV-CT band and the radical band otherwise precludes an accurate band deconvolution and fit. ΔG^0 also was obtained by the fit as well as the ET barrier, ΔG^* . If $C = 0$, ΔG^* depends quadratically on ΔG^0 . If V is zero, ΔG^* will approach ΔG^0 if $\Delta G^0 = \lambda$ and the ground state becomes a single minimum. If V is significant, this will happen for much smaller ΔG^0 as in our case: for **3⁺**, $\Delta G^* \sim \Delta G^0$ and a very shallow second ground state minimum is observed whereas for **4⁺** there is a single minimum ground state.

The IV-CT band energy of **1⁺–4⁺** increases in the series of substituents $R = \text{MeO}, \text{Me}, \text{Cl}$ and CN . This is expected, as the redox asymmetry in **1⁺–4⁺** should increase with decreasing donor strength or increasing acceptor strength, respectively. A plot of ΔG^0 vs. $\Delta E_{1/2} - \Delta E_{1/2}(\mathbf{1})$ (see Fig. 4) is approximately linear ($R = 0.994$) with a slope of 1.36 ± 0.11 . This correlation proves the validity of the Marcus–Hush concept as given in Fig. 1 over a broad energy range (400 mV) as well as the approach of

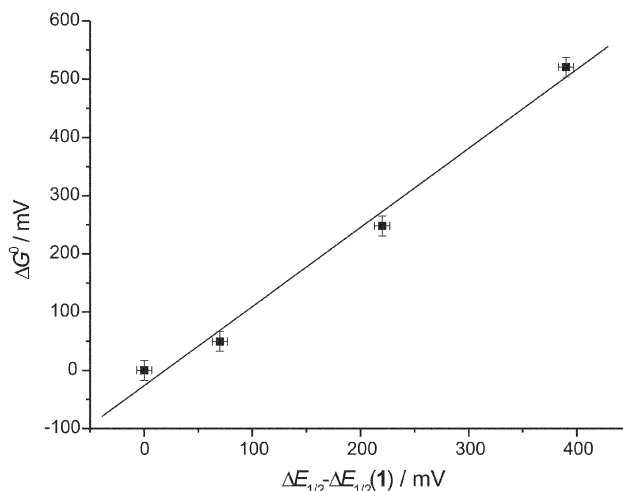


Fig. 4 Correlation of ΔG^0 vs. $\Delta E_{1/2} - \Delta E_{1/2}(\mathbf{1})$ for **1⁺–4⁺** in CH_2Cl_2 –0.2 M TBAH.

scanning ΔG^0 by electrochemical redox splittings. For inorganic MV compounds a linear correlation with slope 1.0 was observed in MeCN and in other polar solvents for a distinctly narrower energy range (*ca.* 250 mV). In contrast, we observed a significantly steeper slope (1.36) in a relatively weakly polar solvent-supporting electrolyte mixture. Unfortunately, we were not able to perform the same measurements in more polar solvent systems owing to solubility problems. In addition, more polar solvents will shift the IV-CT band to higher energy which will increase the band overlap problem drastically.

The reason for the slope being higher than unity is unclear to us. As has been shown above, an increase of V within the series 1^+-4^+ which should enhance $\Delta E_{1/2} - \Delta E_{1/2}(I)$ can be excluded. In any case it should lead to an increase of the redox splitting and to a slope less than unity! Entropy effects have been discussed in the context^{28,34} of these correlations, but as both the redox splitting and ΔG^0 are free energies, entropy should be implicit in this correlation. Another source of possible systematic error is the fact that ΔG^0 refers to the monoradical cation whereas $\Delta E_{1/2}$ involves the thermodynamic properties of both the neutral species and the dication. However, if we disregard the data for 4^+ which are less accurate than those for 1^+-3^+ owing to the strong band overlap we obtain a reasonable slope of 1.16 ± 0.15 with $R = 0.992$ which is much nearer to unity.

Conclusions

We synthesised a series of bis(triarylamine) species whose triarylamine redox centres have different local redox potentials which were tuned by substituents in the *para*-position. The electronic coupling between the redox centres was analysed by the generalised Mulliken-Hush theory which gave a practically constant coupling. All radical cation species show an IV-CT band whose energy varies linearly with the redox potentials splitting. This correlation proves that the Marcus-Hush two-level model is an adequate way to describe the electronic situation in these linear MV systems. The redox asymmetry will help in the design of multidimensional systems with more than two redox centres or redox cascades in which the charge can be located at specific triarylamine moieties.

Experimental

Synthesis

All reactions were performed in flame-dried Schlenk glassware with dry, nitrogen saturated solvents under a nitrogen inert-gas atmosphere. The synthesis of **1** can be found in ref. 6.

***N,N*-Bis(4-methoxyphenyl)-*N',N'*-bis(4-tolyl)tolane-4,4'-diamine 2.** *N,N*-Bis(4-methoxyphenyl)-*N*-(4-ethynylphenyl)amine³⁵ (248 mg, 0.751 mmol), *N,N*-bis(4-tolyl)-*N*-(4-iodophenyl)amine (light sensitive!) (300 mg, 0.751 mmol), PdCl₂(PPh₃)₂ (28 mg, 5 mol%) and CuI (4 mg, 3 mol%) were dissolved in dry diethylamine (15 ml) and stirred at 55 °C for 2 h. The solvent was removed *in vacuo* and the residue was hydrolysed with water. The aqueous phase was extracted with CH₂Cl₂ and the organic phase was dried over Na₂SO₄. After having removed the solvent *in vacuo*, the residue was purified by flash chromatography (silica gel, petroleum ether-CH₂Cl₂ 3 : 2). The crude product was precipitated by slow concentration of a solution in CH₂Cl₂-petroleum ether mixture under reduced pressure. The precipitate was filtered off and dissolved by gentle heating in a little ethyl acetate and precipitated by the addition of petroleum ether which gave a colourless solid (250 mg, 55%), mp 174 °C (Found: C, 83.4; H, 6.1; N, 4.45. Calc. for C₄₂H₃₆N₂O₂: C, 84.0; H, 6.0; N, 4.7%); EI-MS (high resolution, PI): Found: *m/z* 600.2787. Calc. *m/z* 600.2776, $\Delta = 1.8$ ppm; δ_H (250 MHz, CDCl₃) 7.33–7.21 (4H, arom. H), 7.10–6.76 (20H, arom. H), 3.79 (s, 6H, methoxy), 2.31 (s, 6H, methyl); δ_C (63 MHz, CDCl₃)

156.3, 148.5, 147.9, 144.9, 140.5, 133.1, 132.3, 132.2, 130.0, 127.0, 125.1, 121.4, 119.6, 116.0, 114.9, 114.8, 88.9, 88.5, 55.5, 20.8.

***N,N*-Bis(4-methoxyphenyl)-*N',N'*-bis(4-chlorophenyl)tolane-4,4'-diamine 3.** *N,N*-Bis(4-methoxyphenyl)-*N*-(4-ethynylphenyl)amine³⁵ (200 mg, 0.61 mmol), *N,N*-bis(4-chlorophenyl)-*N*-(4-iodophenyl)amine (300 mg, 0.682 mmol), PdCl₂(PPh₃)₂ (40 mg, 9 mol%) and CuI (4 mg, 3 mol%) were dissolved in dry diethylamine and stirred at 55 °C for 12 h. The solvent was removed *in vacuo* and the residue was hydrolysed with water. The aqueous phase was extracted with CH₂Cl₂ and the organic phase was dried over Na₂SO₄. After having removed the solvent *in vacuo*, the residue was purified by flash chromatography (silica gel, petroleum ether-CH₂Cl₂ 3 : 1 → 2 : 3). The crude product was precipitated by slow concentration of a solution in CH₂Cl₂-MeOH mixture under reduced pressure which gave a grey solid (228 mg, 59%), mp 191 °C; EI-MS (high resolution, PI): Found: *m/z* 640.1681. Calc. for C₄₀H₃₀Cl₂N₂O₂ *m/z* 640.1684, $\Delta = 0.3$ ppm; δ_H (400 MHz, CD₂Cl₂) 7.35 (AA', 2H, aminophenyl), 7.26 (AA', 2H, aminophenyl), 7.24 (AA', 4H, chlorophenyl), 7.07 (AA', 4H, methoxyphenyl), 7.02 (BB', 4H, chlorophenyl), 6.97 (BB', 2H, aminophenyl), 6.86 (BB', 4H, methoxyphenyl), 6.80 (BB', 2H, aminophenyl), 3.78 (s, 6H, methoxy); δ_C (101 MHz, CD₂Cl₂) 156.9, 149.1, 147.0, 146.0, 140.4, 132.7, 132.5, 129.8, 127.6, 126.1, 128.8, 123.4, 119.1, 118.3, 115.1, 114.1, 89.9, 88.1, 55.8.

***N,N*-Bis(4-chlorophenyl)-*N*-(4-iodophenyl)amine.** [Bis(trifluoroacetoxy)iodo]benzene (1.13 g, 2.63 mmol) and iodine (660 mg, 2.60 mmol) were stirred in dry chloroform under nitrogen for 1 h at RT. This mixture was dropped under exclusion of light into a solution of *N,N*-bis(4-chlorophenyl)-*N*-phenylamine (1.50 g, 4.33 mmol) in 40 ml of dry chloroform. After having been stirred for 1 h at 50 °C, the mixture was washed with concentrated aqueous Na₂S₂O₃ solution and dried over Na₂SO₄. The solvent was removed *in vacuo* and the residue was purified by flash chromatography (silica gel, petroleum ether-CH₂Cl₂ 15 : 1). The product still contained traces of reactants which we were unable to remove but which did not interfere with the subsequent reactions. Yield 80% colourless solid. δ_H (250 MHz, CD₂Cl₂) 7.54 (AA', 2H, H-3', iodophenyl), 7.22 (AA', 4H, chlorophenyl), 6.99 (BB', 4H, chlorophenyl), 6.80 (BB', 2H, H-2', iodophenyl).

***N,N*-Bis(4-methoxyphenyl)-*N',N'*-bis(4-cyanophenyl)tolane-4,4'-diamine 4.** *N,N*-Bis(4-methoxyphenyl)-*N*-(4-ethynylphenyl)amine³⁵ (120 mg, 0.365 mmol), *N,N*-bis(4-cyanophenyl)-*N*-(4-iodophenyl)amine (150 mg, 0.356 mmol), PdCl₂(PPh₃)₂ (25 mg, 10 mol%) and CuI (3 mg, 4 mol%) were dissolved in dry diethylamine (5 ml) and stirred for 3 h at 55 °C. The solvent was removed *in vacuo* and the residue was hydrolysed with water. The aqueous phase was extracted with CH₂Cl₂ and the organic phase was dried over Na₂SO₄. After having removed the solvent *in vacuo*, the residue was purified by flash chromatography (silica gel, CH₂Cl₂). The crude product was precipitated by slow concentration of a solution in CH₂Cl₂-MeOH mixture under reduced pressure which gave 130 mg (59%) of a yellow solid, mp 117–119 °C; EI-MS (high resolution, PI): Found: *m/z* 622.2368. Calc. for C₄₂H₃₀N₄O₂ *m/z* 622.23905, $\Delta = 3.4$ ppm; δ_H (250 MHz, CD₂Cl₂) 7.55 (AA', 4H, cyanophenyl), 7.49 (AA', 2H, aminophenyl), 7.29 (AA', 2H, aminophenyl), 7.15–7.04 (10H, arom. H), 6.87 (BB', 4H, methoxyphenyl), 6.80 (BB', 2H, aminophenyl), 3.79 (s, 6H, methoxy); δ_C (63 MHz, CD₂Cl₂) 157.1, 150.4, 149.6, 145.0, 140.4, 133.4, 132.7, 134.0, 127.7, 123.8, 126.6, 121.9, 119.1, 119.1, 115.3, 113.7, 106.7, 91.4, 87.6, 55.9.

***N,N*-Bis(4-cyanophenyl)-*N*-(4-iodophenyl)amine.** [Bis(trifluoroacetoxy)iodo]benzene (559 mg, 1.30 mmol) and iodine (304 mg, 1.20 mmol) were stirred in dry chloroform (20 ml)

under nitrogen for 1 h at RT. This mixture was dropped under exclusion of light into a solution of *N,N*-bis(4-cyanophenyl)-*N*-phenylamine (700 mg, 2.37 mmol) in 40 ml of dry chloroform. After having been stirred for 1 h at 50 °C, the mixture was washed with concentrated aqueous Na₂S₂O₃ solution and dried over Na₂SO₄. The solvent was removed *in vacuo* and the residue was purified by flash chromatography (silica gel, CH₂Cl₂). The product was recrystallised from EtOH which gave 680 mg (68%) of light yellow solid, mp 228 °C (Found: C, 57.0; H, 2.9; N, 10.0. Calc. for C₂₀H₁₂IN₃: C, 57.0; H, 2.9; N, 10.0%). δ_H (250 MHz, CDCl₃) 7.69 (AA', 2H, H-3', iodophenyl), 7.54 (AA', 4H, cyanophenyl), 7.11 (BB', 4H, cyanophenyl), 6.88 (BB', 2H, H-2', iodophenyl); δ_C (63 MHz, CDCl₃) 149.8, 145.0, 139.4, 133.7, 128.3, 123.3, 118.6, 106.6, 90.3.

Cyclic voltammetry and spectroelectrochemistry

The electrochemical experiments were performed in dry, nitrogen-saturated CH₂Cl₂ with 0.2 M tetrabutylammonium hexafluorophosphate (TBAH) as supporting electrolyte and 0.001 M substrate using a conventional three-electrode set-up with a platinum disk electrode. The potentials are referenced against ferrocene (Fc/Fc⁺). Digital fits of the experimental CVs were done with DigiSim³⁶ with the assumption of chemical and electrochemical reversibility of all processes. For spectroelectrochemical analysis, the solutions of the CV experiments were transferred into a thin-layer cell which comprised two quartz windows with a gold mini-grid working electrode squeezed in-between. The optical path length was 100 μm. The cell design has been described elsewhere.³⁷ The UV/Vis/NIR spectra were recorded with a Perkin-Elmer lambda-9 spectrometer in transmission mode.

Acknowledgements

This work was supported by the Fonds der Chemischen Industrie and the Deutsche Forschungsgemeinschaft. We thank Professor J. Daub for kind support during the work in Regensburg.

References

- 1 D. P. West and M. D. Rahn, in *Photorefractive Materials*, ed. V. Balzani, Wiley-VCH, Weinheim, 2001.
- 2 M. Grätzel and J.-E. Moser, in *Solar Energy Conversion*, ed. V. Balzani, Wiley-VCH, Weinheim, 2001.
- 3 J. C. Scott and G. G. Malliaras, in *The Chemistry, Physics and Engineering of Organic Light-Emitting Diodes*, ed. G. Hadziioannou and P. v. Hutten, Wiley-VCH, Weinheim, 2000.

- 4 C. Lambert and G. Nöll, *Angew. Chem., Int. Ed.*, 1998, **37**, 2107.
- 5 C. Lambert, W. Gaschler, E. Schmäzlin, K. Meerholz and C. Bräuchle, *J. Chem. Soc., Perkin Trans. 2*, 1999, 577.
- 6 C. Lambert and G. Nöll, *J. Am. Chem. Soc.*, 1999, **121**, 8434.
- 7 C. Lambert, G. Nöll and F. Hampel, *J. Phys. Chem. A*, 2001, **105**, 7751.
- 8 C. Lambert and G. Noll, *Chem. Eur. J.*, 2002, **8**, 3467.
- 9 J. Bonvoisin, J.-P. Launay, W. Verbouwe, M. Van der Auweraer and F. C. De Schryver, *J. Phys. Chem.*, 1996, **100**, 17079.
- 10 J. Bonvoisin, J.-P. Launay, M. Van der Auweraer and F. C. De Schryver, *J. Phys. Chem.*, 1994, **98**, 5052.
- 11 V. Coropceanu, M. Malagoli, J. M. André and J. L. Brédas, *J. Am. Chem. Soc.*, 2002, **124**, 10519.
- 12 C. Creutz, *Prog. Inorg. Chem.*, 1983, **30**, 1.
- 13 R. J. Crutchley, *Adv. Inorg. Chem.*, 1994, **41**, 273.
- 14 B. S. Brunschwig, C. Creutz and N. Sutin, *Chem. Soc. Rev.*, 2002, **31**, 168.
- 15 S. F. Nelsen, J. Adamus and J. J. Wolff, *J. Am. Chem. Soc.*, 1994, **116**, 1589.
- 16 S. F. Nelsen, R. F. Ismagilov and D. A. Trieber, *Science*, 1997, **278**, 846.
- 17 S. Mazur, C. Streekumar and A. H. Schroeder, *J. Am. Chem. Soc.*, 1976, **98**, 6713.
- 18 F. A. Neugebauer, S. Bamberger and W. R. Groh, *Chem. Ber.*, 1975, **108**, 2406.
- 19 S. Dapperheld, E. Steckhan, K.-H. G. Brinkhaus and T. Esch, *Chem. Ber.*, 1991, **124**, 2557.
- 20 B. S. Brunschwig and N. Sutin, *Reflections on the Two-state Electron-transfer Model*, ed. V. Balzani, Wiley-VCH, Weinheim, 2001.
- 21 N. S. Hush, *Coord. Chem. Rev.*, 1985, **64**, 135.
- 22 S. F. Nelsen, R. F. Ismagilov and D. R. Powell, *J. Am. Chem. Soc.*, 1997, **119**, 10213.
- 23 S. F. Nelsen, R. F. Ismagilov, K. E. Gentile and D. R. Powell, *J. Am. Chem. Soc.*, 1999, **121**, 7108.
- 24 R. A. Marcus, *J. Phys. Chem.*, 1989, **93**, 3078.
- 25 S. F. Nelsen, *Chem. Eur. J.*, 2000, **6**, 581.
- 26 F. Barrière, N. Camire, W. E. Geiger, U. T. Mueller-Westerhoff and R. Sanders, *J. Am. Chem. Soc.*, 2002, **124**, 7262.
- 27 Y. J. Chen, C.-H. Kao, S. J. Lin, C.-C. Tai and K. S. Kwan, *Inorg. Chem.*, 2000, **39**, 189.
- 28 J. P. Chang, E. Y. Fung and J. C. Curtis, *Inorg. Chem.*, 1986, **25**, 4233.
- 29 M. D. Newton, *Adv. Chem. Phys.*, 1999, **106**, 303.
- 30 C. Creutz, M. D. Newton and N. Sutin, *J. Photochem. Photobiol. A: Chem.*, 1994, **82**, 47.
- 31 R. J. Cave and M. D. Newton, *Chem. Phys. Lett.*, 1996, **249**, 15.
- 32 S. F. Nelsen and F. Blomgren, *J. Org. Chem.*, 2001, **66**, 6551.
- 33 S. F. Nelsen and M. D. Newton, *J. Phys. Chem. A*, 2000, **104**, 10023.
- 34 R. A. Marcus and N. Sutin, *Comments Inorg. Chem.*, 1986, **5**, 119.
- 35 C. Lambert, G. Nöll, E. Schmalzlin, K. Meerholz and C. Bräuchle, *Chem. Eur. J.*, 1998, **4**, 2129.
- 36 M. Rudolph and S. W. Feldberg, DigiSim 3.03a, Bioanalytical Systems, Inc., 1994–2000.
- 37 J. Salbeck, *Anal. Chem.*, 1993, **65**, 2169.